Recent advances in the application triplet–triplet annihilation-based photon upconversion systems to solar technologies

Jacopo Pedrini
Angelo Monguzzi

SPIE.

Recent advances in the application triplet–triplet annihilation-based photon upconversion systems to solar technologies

Jacopo Pedrini and Angelo Monguzzi*

Università degli Studi Milano-Bicocca, Dipartimento di Scienza dei Materiali, Milano, Italy

Abstract. Upconversion (UC) of low-energy photons into high-energy light can in principle increase the efficiency of solar devices by converting photons with energies below the energy absorption threshold into radiation that can be utilized. Among UC mechanisms, the sensitized triplet–triplet annihilation-based upconversion (sTTA-UC) is the most recent that would be applied in solar technologies. sTTA-UC was demonstrated using sunlight in 2006, and due to its high efficiency at low excitation intensities with noncoherent light, it is considered a promising strategy for the recovering of subbandgap photons. Here, we describe briefly the working principle of the sTTA-UC, and we review the most recent advances of its use in solar applications. © *The Authors. Published by SPIE under a Creative Commons Attribution 3.0 Unported License. Distribution or reproduction of this work in whole or in part requires full attribution of the original publication, including its DOI.* [DOI: 10.1117/1.JPE.8.022005]

1 Introduction

The Shockley–Queisser model for single-junction solar cells (SCs) states that the efficiency of a single-junction device depends on the bandgap of the reactive material. This is a direct consequence of the fact that photons of lower energy than the semiconductor bandgap cannot be absorbed, while charges created after absorption of photons of higher energy than the bandgap undergo thermalization.[1] Since all solar devices feature this intrinsic absorption energy threshold, incident photons with energies below this threshold do not contribute significantly to current generation in the SC. These losses are called transmission or subbandgap losses.[2] The extent of the losses is shown in Fig. 1(a) for different single-junction SC technologies.

Upconversion (UC) of low-energy photons into high-energy light can in principle increase the efficiency of solar devices by converting photons with energies below the energy absorption threshold into radiation that can be utilized. In their theoretical study, more recently confirmed and developed by Atre and Dionne,[3] Trupke et al.[4] showed that a system consisting of a SC with a single bandgap of 2 eV and an ideal upconverter coupled to its rear can achieve a maximum power conversion efficiency of 47.6% under nonconcentrated sunlight. Since (i) this efficiency value is remarkably higher than the Shockley–Queisser limit of 34% for devices with a bandgap of 1.34 eV and (ii) upconverters can be in principle easily implemented in existing technologies, in the last decade many efforts have been made by the scientific community towards the development of efficient upconverters for real-world solar technologies.[5]

Among UC mechanisms, the sensitized triplet–triplet annihilation-based upconversion (sTTA-UC) is the most recent photon UC technique to be potentially applied to solar technologies.[6] sTTA-UC has been demonstrated with sunlight by Baluschev et al.,[7] and due to its high efficiency at low excitation intensities with noncoherent light, it is indeed considered a very promising strategy for the recovery of subbandgap photons in photovoltaic and

---

*Address all correspondence to: Angelo Monguzzi, E-mail: angelo.monguzzi@unimib.it
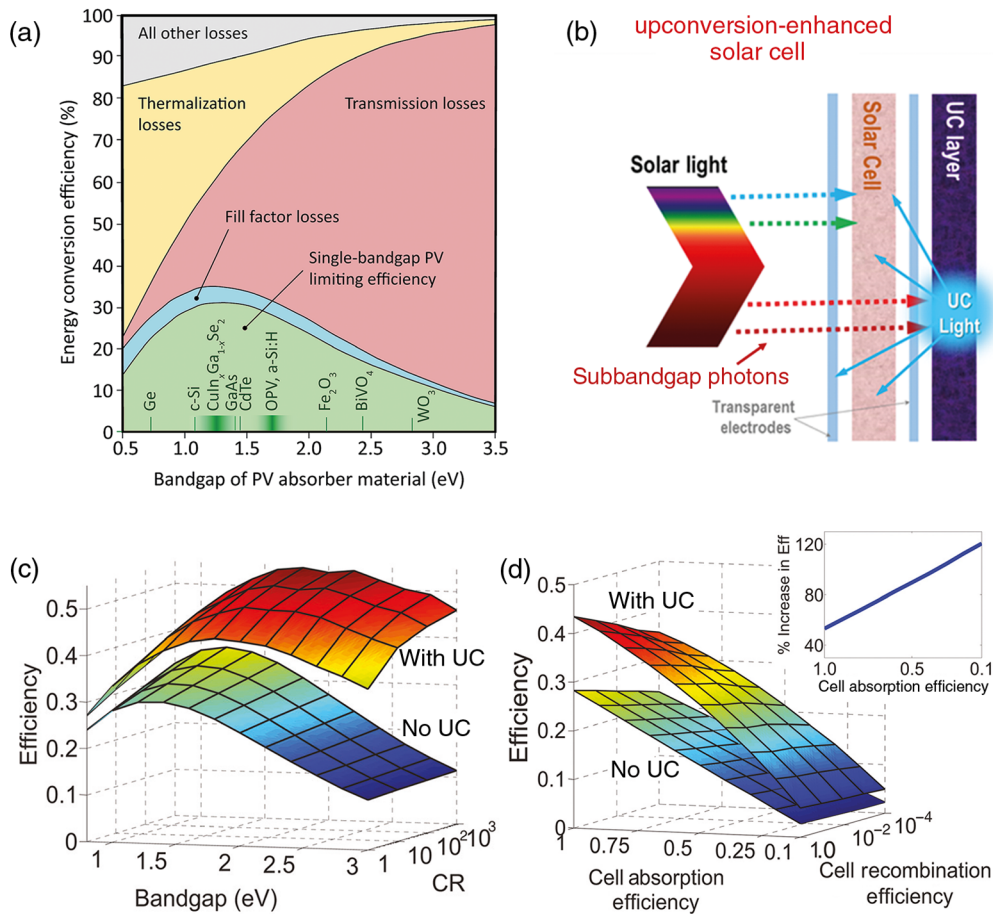
Fig. 1 (a) Relative importance of fundamental loss mechanisms in solar energy conversion as a function of the PV absorber semiconductor bandgap and examples of absorber materials, plotted for a 6000-K spectrum. Reproduced from Ref. 2 with permission from The Royal Society of Chemistry. (b) Conceptual sketch of a UC-enhanced solar device. (c) The calculated absolute efficiency of an SC as a function of cell bandgap and light concentration ratio both with and without an ideal upconverter UC. (d) Absolute efficiency versus the absorption efficiency and recombination efficiency of the SC, both with and without an upconverter UC calculated for device with bandgap 1.7 eV and relaxation energy of 300 meV. (Inset) The relative increase in efficiency is larger for a poorly absorbing SC but is essentially independent of SC recombination efficiency. Reproduced from Ref. 3, with the permission of AIP Publishing.

photocatalytic devices working under the solar irradiance.[2,8] In the following, we describe the working principle of the sTTA-UC and review the most recent advances of its application to solar technologies.

1.1 Principles of Sensitized Triplet–Triplet Annihilation-Based Upconversion

UC of low-energy photons from a noncoherent radiation source, such as the sun, is most frequently a multistep process that involves the sensitized population of metastable optically dark electronic states of a given system.[5] These can transit to higher emissive states by receiving additional energy through energy transfer (ET) from other sensitizers (ions or molecules) or by mutual annihilation upon biexcitonic collisions. The radiative transition from the reached higher energy level to the ground state leads to the emission of the desired higher energy photon. There are two main reasons why most frequently an ET process is involved: first, it is not necessary that one sort of ion or molecule provides all needed energy levels; second, an excited ion or molecule does not have to absorb more than one photon, which would be an extremely unlikely event requiring high excitation intensity.
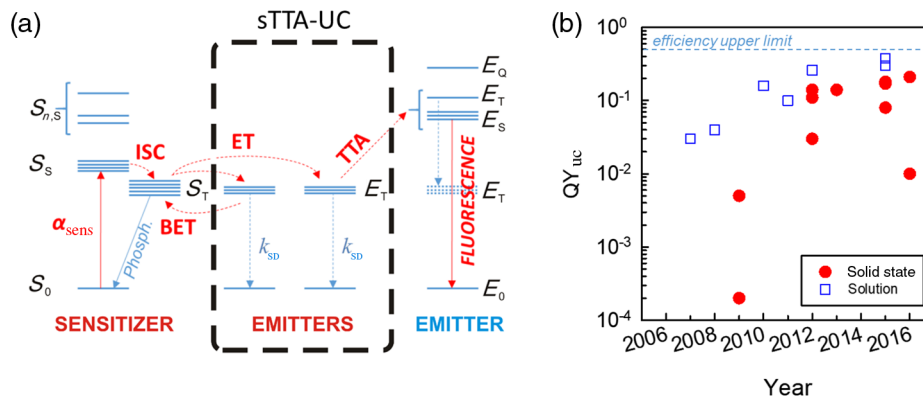
Fig. 2 (a) Energy-level diagram for the sTTA-UC process. A sensitizer with absorptance α_{sens} is excited into a singlet state (S_S) that efficiently undergoes intersystem crossing (ISC) into the triplet state (S_T). ET then competes with back energy transfer (BET) to E_T. These E_T can either sponta-neously decay (with a rate constant k_{SD}) or undergo TTA to an excited singlet state of the emitter (E_S). Emitter quintet states (E_Q) are not energetically accessible. (b) Evolution of sTTA-UC quantum efficiency QY_{uc} from its demonstration with sunlight in 2006, both in liquid- [Refs. 13 and 14–20] and solid-state environment [Refs. 21–29]. The dashed line marks the theoretical upper limit of 50% in the UC process.

Indeed, to realize devices working under standard solar irradiance, traditional UC mecha-nisms, such as second-harmonic generation or sequential multiphoton absorption by lanthanide ions, are still not suitable because they require coherent and/or high-intensity irradiation to reach high efficiencies.[5,9] Conversely, the sTTA-UC also occurs at excitation intensities as low as a few mW cm^{-2} and exhibits quantum efficiencies (QY_{uc}) at low power that are orders of magnitude higher than those of the aforementioned processes.[10–12] In this multistep UC route, energy absorbed by a sensitizer is transferred to a second moiety, the emitter, by means of a trip-let–triplet ET process. Subsequently, two optically dark emitter triplets (E_T) undergo triplet–trip-let annihilation (TTA) to produce one excited singlet state, from which a photon with higher energy than those absorbed is emitted [Fig. 2(a)]. Since its demonstration in solution with con-centrated sunlight and thanks to its surprisingly high efficiency at low powers, materials for sTTA-UC have been intensively studied and developed to achieve higher performances and to cover a larger fraction of the visible (Vis)–near-infrared (NIR) spectrum.[7,12,30–32] By choosing the proper emitter/sensitizer pair, UC quantum efficiencies (QY_{uc}) above 30% have been obtained at excitation power densities of 10s of mW cm^{-2}. This remarkable value is not far from the maximum theoretical yield of 50% arising from the energy conservation law.[13,33] Figure 2(b) shows the gradual increment of QY_{uc} achieved in the last 10 years. Notably, despite a slower initial development, a good performance is now assessed even for solid-state materials. Nowadays, the research on sTTA-UC for solar applications is indeed focused on the design and development of solid systems that match the strict requirements for technological applications. The crucial issue for solid sTTA-UC is to keep the proper mixing of sensitizer and emitter moieties while maintaining the exciton diffusivity that maximizes the ET and the TTA steps as in low-viscosity solutions. If these requirements are met, the excitation intensity threshold I_{th} required to obtain the maximum QY_{uc} can be achieved below the solar irradiance, thus allowing for the design and development of UC-assisted devices.[34] However, despite several materials based on polymers,[21,35–38] supramolecular gels,[39–41] organic[42] or polymeric[22,43] glasses, and hybrid nanocrystal/dye films[23] showed interesting performances at low powers, examples of prototype solar devices are still in the embryonal state.

2 Sensitized Triplet–Triplet Annihilation-Based Upconversion in Photovoltaics

Despite being known for about 50 years,[44] sTTA-UC was experimentally demonstrated with concentrated sunlight in 2006 by Baluschev et al., and, successively, it has been coupled to
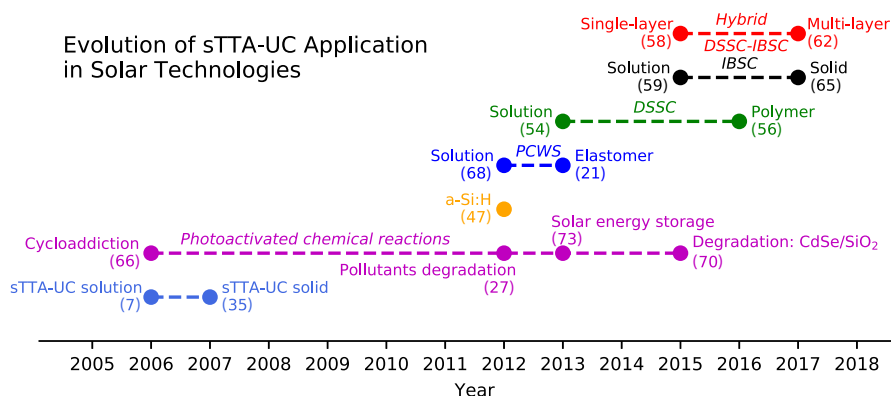
Fig. 3 Timeline of the technological advances for the application of sTTA-UC to solar energy devices.

several types of SCs, as shown in Fig. 3, which summarizes the most important milestones and advances in the development of sTTA-UC materials and applications in solar technologies. In the following, we describe the state-of-the-art of UC-coupled SCs that exploit the sTTA-UC mechanism to improve their photon-harvesting ability. The text is organized in several sections, according to the type of semiconductor material employed to harvest the incoming radiation.

2.1 Silicon-Based Devices

The Australian research group lead by Schmidt[2,45,46] is a pioneer in the sTTA-UC field not only for the deep study of the fundamental photophysics occurring in the process but also for the development of numerical models and prototype devices that describe and exploit the sTTA-UC. In particular, they focused on the efficiency enhancing of silicon-based SC cells, the most diffuse solar devices commercially available. In 2012, they reported the first integrated a-Si:H/TTA-UC photovoltaic device as a proof-of-principle of a third-generation device, and they demonstrated how to characterize such an upconversion-enhanced solar cell (UC-SC) so that its performance under solar conditions may be evaluated.[47] As shown in Fig. 4, they realized a multilayer device based on the use of a thin bifacial a-Si:H p-i-n cell coupled to a sTTA-UC solution where the tetrakisquinoxalinoporphyrin (PQ_4Pd) and its derivative PQ_4PdNA were used as sensitizers and rubrene as an annihilator/emitter moiety for NIR-to-VIS UC. With a 50-nm-thick UC-SC, they observed an overall relative energy conversion efficiency increase of about 0.1% under 48 suns of noncoherent white excitation.

A following improvement of the device architecture lead to an enhancement of ~0.2% under 19 suns,[48] a value further enlarged with the inclusion of a back reflector to improve the harvesting of the upconverted light by the silicon layer.[49]

2.2 Organic and Hybrid Devices

The electronic properties of the most efficient sTTA-UC pairs allow for the exploitation of light in the NIR and Vis spectral ranges. Therefore, it is not difficult to imagine that these systems can be coupled with a SC with an energy bandgap wider than silicon as dye-sensitized solar cells (DSSC). DSSCs are a photovoltaic technology that has generated significant interest across a broad range of research fields since their first report.[50] Unfortunately, despite the large effort made, the highest reported device efficiencies remain relatively low. However, this is partially compensated for by low projected manufacturing costs and their strong performance in ambient and diffuse lighting conditions.

The large driving forces required for effective charge transfer in DSSCs necessitate the use of absorbers with large absorption thresholds.[51,52] This large energy gap, therefore, results in a significant section of the solar spectrum remaining unused by the cell, which can be recovered using a suitable UC system.[53] In 2013, Nattestad et al.[54] demonstrated that a DSSC cell displays
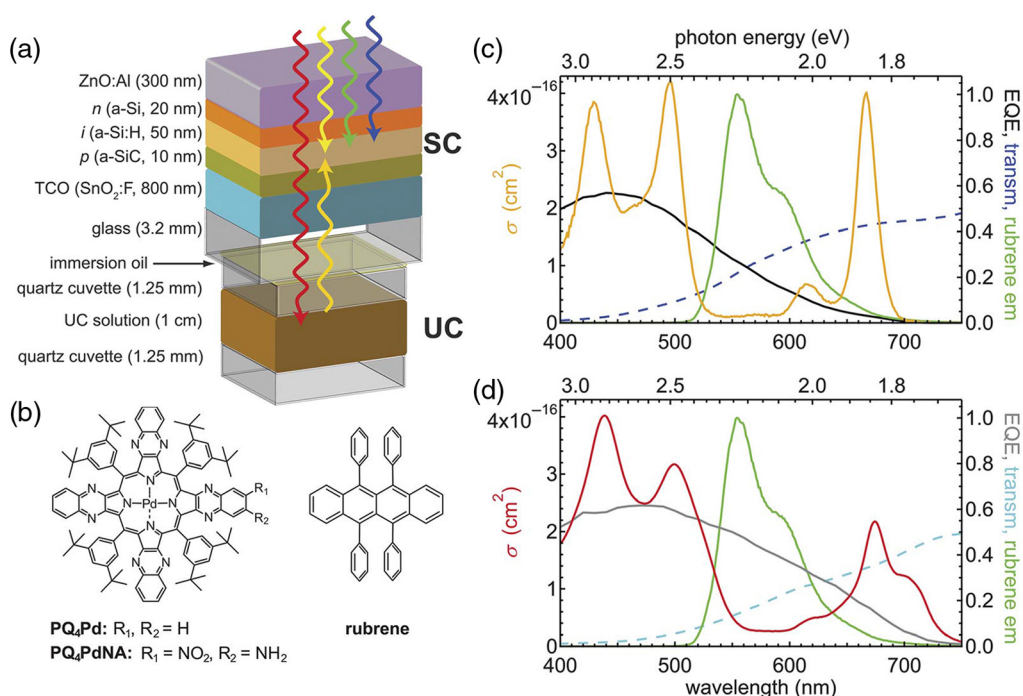
Fig. 4 (a) An illustration of the integrated a-Si:H *p-i-n*/UC device. Low-energy (shown in red) photons pass though the *p-i-n* structure and excite dye molecules in the UC unit, which subsequently returns photons of a shorter wavelength (yellow). (b) The molecules utilized for photochemical UC: two Pd porphyrins, PQ_4Pd and PQ_4PdNA, were employed as sensitizers in combination with the highly efficient TTA emitter rubrene. (c, d) Spectral characterization: comparison of the EQE (black for 50 nm, gray for 100-nm *i*-layer) and transmission curves (dashed) of the respective a-Si:H SC with the absorption cross section (s, orange or red) and emission (green) profile of the UC unit constituents. (c) 50-nm a-Si:H SC and PQ_4Pd, (d) 100-nm a-Si:H SC and PQ_4PdNA. Reproduced from Ref. 47 with permission from The Royal Society of Chemistry.

enhanced current under subbandgap illumination at a low light concentration (3 suns) when an SC has been coupled to the a PQ_4PdNA/rubrene solution, whose upconverted emitted photons are recaptured by the D149 dye.

In 2016, a significant step forward in this research was made by Akindoyo et al.,[55] who presented a study where, for the first time, the sTTA-UC enhancement of an SC performance is combined with the ability to embed the chromophores in polymer matrices that can be tailored to films and many different shapes and sizes. The synthetic flexibility and longevity of these sTTA-UC films are of the utmost importance for economically practical applications. The films are indeed robust against oxygen quenching and can be readily tailored to existing SC architectures [Fig. 5(a)]. The photovoltaic performance of the UC-assisted DSSC device [Figs. 5(b) and 5(c)] was measured under both high-power coherent laser and low-power incoherent light irradiation.[56] The resulting photovoltaic performance is summarized in Fig. 5(c). In a DSSC based on a 5-μm-thick mesoporous TiO_2 layer and a single sTTA-UC film, the short-circuit photocurrent J_{sc} was enhanced by 13.6% and 20.3% upon illumination with the equivalent of 1 sun and 2 suns, respectively. The addition of a rear reflector to utilize more effectively the upconverted photons almost doubles the J_{sc} enhancement observed.

An alternative device architecture for UC-enhanced DSSC was proposed by the group lead by Hanson in 2015, inspired by the concept of intermediate band cells (*vide infra*, Sec. 2.3).[57] To facilitate the sTTA-UC and the charge separation of the upconverted excitons, they used an inorganic−organic interface based on self-assembled bilayers of a TTA molecular pair on metal oxide surfaces. This self-assembled motif via metal ion linkages is shown in Fig. 6(a) and provides a simple and modular method for multimolecular assembly on a metal oxide surface.[58,59] This strategy is not diffusion limited and offers unprecedented geometric and spatial control of
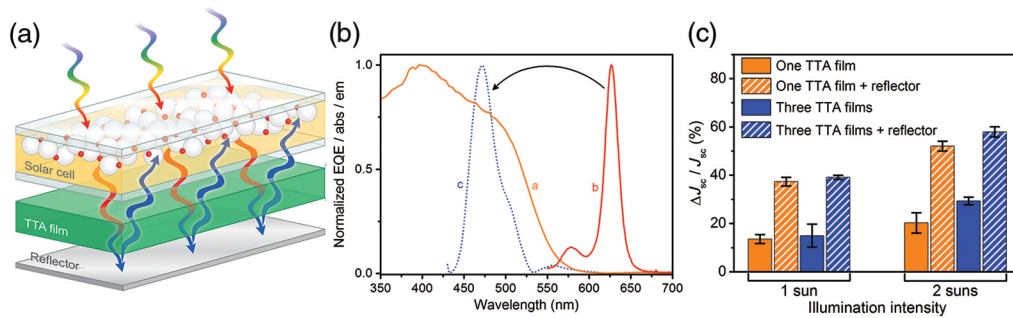
Fig. 5 (a) Schematic illustration of sTTA-UC film-assisted absorption of photons with energies below the HOMO–LUMO gap of the chromophore sensitizer D131 employed in a DSSC device. (b) Normalized (yellow) external quantum efficiency spectrum of a D131-sensitized TiO_2 photo-electrochemical cell, (red) Q-band absorption of PdTPBP, and (blue) UC-emission spectrum of a sTTA-UC film. (c) sTTA-UC induced the short-circuit current density (J_{sc}) enhancement using an LED source (625 nm) illumination of the DSSC device with 5-μm sensitized TiO_2 layer. Error bars represent standard deviation of five measurements. Reprinted with permission from Ref. 56. Copyright 2016 American Chemical Society.

the donor−acceptor interactions at an interface. The bilayer film depicted is prepared by stepwise soaking of nanocrystalline TiO_2 or ZrO_2 films in three separate solutions of 4,4′-(anthracene-9,10-diyl)bis(4,1-phenylene)diphosphonic acid (DPPA), $Zn(CH_3COO)_2$, and Pt(II)tetrakis(4-carboxyphenyl)porphyrin (PtTCPP). Anthracene and platinum porphyrin derivatives were selected as the TTA-UC pair because they are known to exhibit efficient UC-emission. Figure 6(b) shows the electronic transitions and relative energetics for DPPA and PtTCPP and the conduction band (CB) energies of TiO_2 and ZrO_2. The authors demonstrated the generation of photocurrent with subbandgap photons by monitoring the peak photocurrent for TiO_2-DPPA-Zn-PtTCPP with respect to 532-nm excitation. The photocurrent density exhibits a change in slope from 1.2 to 0.61 that is reminiscent of the quadratic to linear behavior typical for sTTA-UC [Fig. 6(c)]. This change in slope is in contrast to that for TiO_2-PtTCPP, which exhibits a slope of 0.53 throughout the entire excitation intensity range from ~300 to 7000 mW cm^{-2}. Under the same conditions, a similar linear dependence (slope = 0.5) is observed for the common DSSC dye employed N3, which is known to undergo a one photon-to-one electron photocurrent generation mechanism.[60] By combining intensity dependence and incident photon-to-electron conversion efficiency measurements, they further demonstrated that these bilayer films effectively generate a photocurrent by two different mechanisms: (1) direct excitation and electron injection from the acceptor molecule and (2) low-energy light
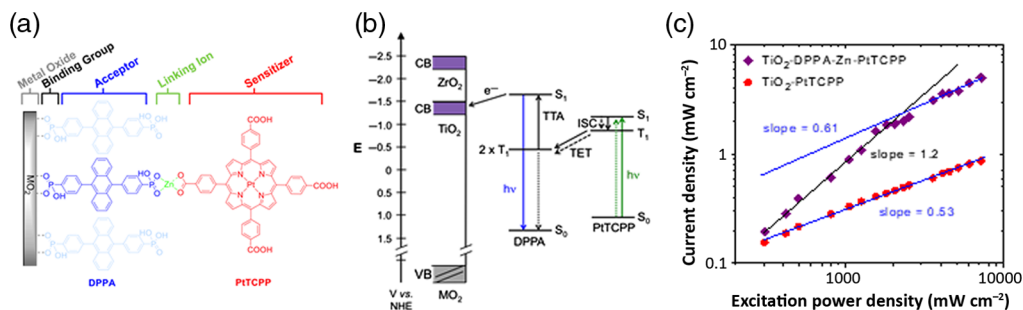

Fig. 6 (a) Chemical structure of DPPA and PtTCPP and a schematic representation of the bilayer film on a metal oxide surface (MO_2-DPPA-Zn-PtTCPP). (b) Electronic transitions and relative energetics for DPPA and PtTCPP and the CB energies of TiO_2 and ZrO_2. (S_n = singlet state, T_n = triplet state, ISC = intersystem crossing, TET = triplet energy transfer, TTA = triplet−triplet annihilation). (c) Peak photocurrent density from TiO_2-DPPA-Zn-PtTCPP and TiO_2-PtTCPP with respect to 532-nm excitation intensity. (TiO_2 thin film working electrode, platinum counter electrode, 0.3 M TBAClO4 in N_2 deaerated MeCN electrolyte at 0-V applied potential). Reproduced from Ref. 58 with permission from The Royal Society of Chemistry.
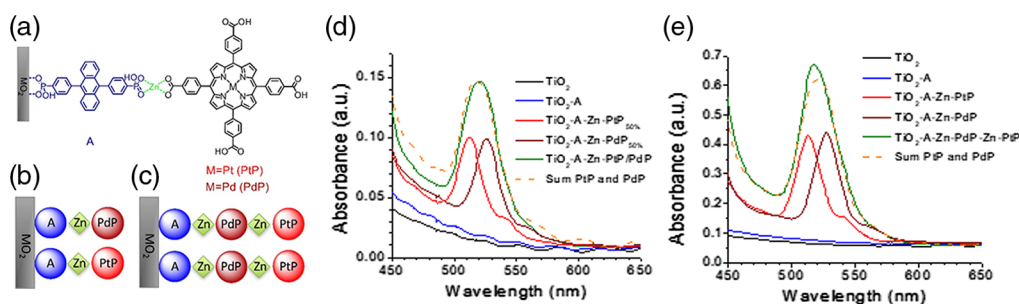
Fig. 7 (a) Structure of the emitter A, and sensitizers PtP, and PdP molecules with the schematic representation of (b) the dual sensitized bilayer and (c) dual sensitized trilayer films. (d) Absorption spectra for the dual sensitized bilayer and trilayer as well as (e) their constituent single sensitizer films on TiO$_2$. The calculated spectra, from the scaled sum of the single sensitized films, are shown as dashed orange lines. Reprinted with permission from Ref. 62. Copyright 2017 American Chemical Society.

absorption by the sensitizer molecule followed by sTTA-UC and electron injection from the upconverted state. Notably, the power conversion efficiency from the upconverted photons is the highest yet reported for an SC integrated with sTTA-UC.[61]

Further developing this strategy, to overcome the intrinsic limitation of porphyrin-like sensitizers, i.e., their narrow absorption bandwidth that limits the system absorptance, Dilbeck et al.[62] recently introduced a trilayer architecture as a new system for incorporating multiple sensitizers into sTTA-UC film-based DSSC (Fig. 7). By means of interlayer ET from both sensitizers in the bilayer, and in energy cascade for the trilayer, it is possible to efficiently absorb low-energy light and generate acceptor triplet-excited states. A photocurrent enhancement is observed in the multisensitizer films due to cooperative broadband absorption of employed light harvesters. The efficiency of the trilayer device ($1.2 \times 10^{-3}\%$), with high sensitizer density and directional ET that cascades toward the charge separation interface, marks another record among the performance of integrated sTTA-UC-SCs currently reported. Importantly, intensity dependence measurements demonstrate that high triplet densities and peak UC efficiency can be achieved at subsolar irradiance using dual sensitized self-assembled multilayer films. Even though the device efficiency is still low, these results suggest that an integrated sTTA-UC DSSC offers a viable means of enhancing solar energy harvesting efficiencies upon several improvements, including optimizing overlap between the sensitizer(s) and the solar spectrum, increasing injection yield from the singlet-excited state of the acceptor molecule, maximizing the regeneration rate, and reducing the triplet quenching losses.

2.3 Intermediate Band Solar Cells

Intermediate band solar cells (IBSCs) are a third-generation SC technology where, as the name suggests, the inclusion of an absorbing band in the energy gap of the "main" semiconducting material allows for the increase in the efficiency, potentially exceeding the Shockley–Queisser limit. The new band opens a second absorption channel; therefore, the photoexcitation of carriers into the CB can occur from direct absorption from the valence band (VB) or after consequent absorption of lower energy photons from the VB to the intermediate band (IB) and then from the IB to the CB.

The fabrication of IBSCs has always been limited by strict constraints of the intermediate absorption band, namely (i) a generally low-absorption cross section, (ii) the need to use spectrally selective absorbers, i.e., to avoid the excitation of carriers to the IB *via* a higher energy photon, and (iii) the rapid nonradiative relaxation from the IB to the VB. Organic IBSCs based on sTTA-UC allow overcoming all the above constraints by exploiting the unique electronic structures of the employed components. In detail, the extremely high molar extinction coefficient of metalated porphyrins allows for high absorption of light, while the narrow absorption peak selects only the wavelengths that will be used to activate the TTA process. Simultaneously, the E_T that are populated *via* TTA are metastable dark states with an extremely low oscillator
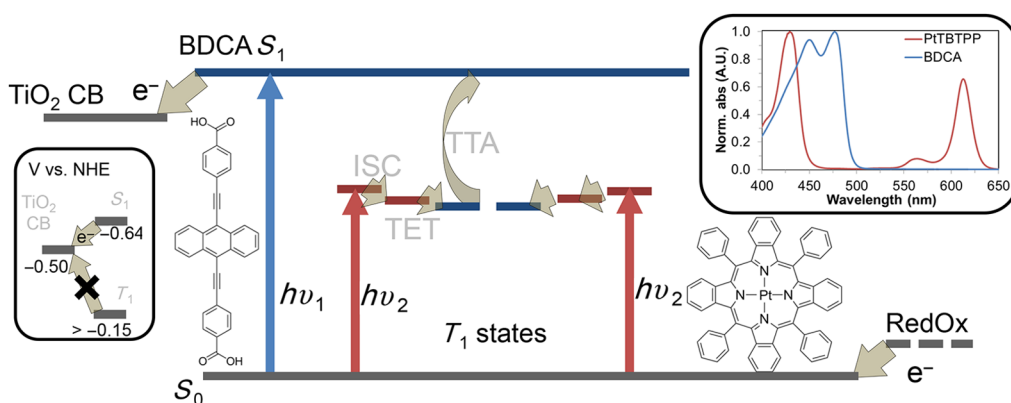
Fig. 8 Energy-level diagram of an IBSC, with excitation of BDCA (left structure, blue states) occurring either by direct excitation with a single high-energy photon ($h\nu_1$) or by two low-energy photon ($h\nu_2$) absorptions, commencing with photoexcitation of PtTBTPBP (right structure, red states). Left inset demonstrates energetically favorable electron injection into the TiO$_2$ CB from BDCA (S_1) but not BDCA (T_1), while the right inset shows the absorption spectra of PtTBTPP and BDCA (measured in DMF). Reproduced from Ref. 59 with permission from The Royal Society of Chemistry.

strength that makes them very long-lived and avoids fast nonradiative relaxation. For all these reasons, IBSCs based on sTTA-UC are a new, exciting class of devices potentially able to harvest subbandgap photons.

The concept of IBSCs was presented in 1997 by Luque and Martí,[63] while the idea of fabricating an organic IBSC based on sTTA-UC first came by Ekins-Daukes and Schmidt[64] in 2008. They demonstrated that the most efficient electronic structure for an sTTA-UC IBSC features a symmetrical band structure arrangement, with the IB lying at around midgap. The power conversion efficiency has been calculated to be up to 40.6% for 1.9-eV excitation light under 1-sun illumination, exceeding the Shockley–Queisser limit. However, no significant IBSC has been fabricated until very recently.[2] The first TTA-UC-based IBSC was demonstrated by Simpson et al.[59] in 2015 by staining a screen-printed commercial TiO$_2$ paste with an upconverting solution composed of Pt(II)-tetrabenzotetraphenylporphyrin (PtTBTPP, the sensitizer) and 4,4′-(anthracene-9,10-diylbis(ethyne-2,1-diyl))dibenzoic acid (BDCA, the emitter). The energy-level schematic of the prototype devices is shown in Fig. 8. This IBSC is shown to generate photocurrent when illuminated with incoherent light whose energy is well below the bandgap of TiO$_2$ (560 nm $< \lambda <$ 640 nm), while a control device with no BDCA showed no photocurrent under the same conditions.

A different approach to sTTA-UC-based IBSCs has been recently given by Lin et al.[65] They fabricated an all-solid-state organic cell with the active layer composed of a blend of PtTPTBP and α-sexithiophene (α-6T) as the sensitizer and emitter, respectively. The acceptor layer for the IBSC was diindenoperylene and was compared with C60, which has a charge transfer state with a much lower energy than the triplet states of α-6T. Therefore, the cell with C60 has a direct funneling of charges from α-6T triplets to C60, bypassing TTA and serving as a model, control system. With their IBSC, the authors were able to reach a 12% increase in photocurrent with respect to the control system under subbandgap illumination intensity lower than 0.1 mW cm^{-2}. The examples reported above are interesting and promising steps forward to the realization of efficient IBSC based on sTTA-UC due to its photophysical properties that overcome the major limitations of this SC technology.

3 Sensitized Triplet–Triplet Annihilation-Based Upconversion in Photochemical Systems

Beyond improving SC efficiencies, the sTTA-UC can also be used to enable photochemical reactions, many of whose require high-energy photons, generally blue or UV, which are scarce in the solar spectrum. Taking into account that the spectral range where sTTA-UC is more

efficient is from the Vis to the near-UV, the expected response to the coupling with an upconverter is expected to be greater for these systems than that of SCs.

In 2006, Islangulov and Castellano[66] demonstrated that bimolecular cycloaddition between two anthracene molecules was possible even when excited with light that anthracene itself does not absorb due to the exploitation of a proper sensitizer. In this study, there was no need for the emitter to radiate a photon, as it is the singlet-excited acceptor produced in the TTA step that reacts further. This was the first example representing a larger group of synthetic applications where reactions requiring high-energy UV–blue photons can be promoted by UC mechanisms, either where the produced excited singlet acceptor is the reacting species, as above, or where the emitted photon from the excited singlet acceptor in turn excites the reacting specimen.

In addition to the traditional photochemistry, the sTTA-UC is especially suited to be coupled with water-splitting cells that exploit wide-bandgap photocatalysts, since currently such catalysts cannot utilize about 95% of the available solar photons.[67] sTTA-UC-enhanced photo-catalytic water splitting (PCWS) was demonstrated in 2012 under noncoherent irradiation in a proof-of-principle photoelectrochemical device (Fig. 9).[68] The blue photons emitted from a quartz cuvette containing 9,10-diphenylanthracene (DPA) and palladium(II)-octaethylporphyrin (PdOEP) upconverting solution were used to activate the water-splitting reaction driven by a tungsten trioxide (WO_3) photoanode under low-energy excitation ($\lambda > 500$ nm), well below the low-energy absorption tail of WO_3 (450 nm). Kim et al. developed this approach successively with a Pt-loaded WO_3 (Pt/WO_3) photocatalyst. Once irradiated with photons of energy above its bandgap ($\lambda < 440$ nm), it produces hydroxyl radicals ($\cdot$ OH).[27] The sTTA-UC enabled the photoassisted production using subbandgap green photons (532 nm). In this case, the photon UC was achieved directly in the aqueous phase by encapsulating the solvent phase containing the DPA/platinum(II)-octaethyl-porphyrin (PtOEP) benchmark sensitizer/emitter pair in a rigid polymer shell in the form of aqueous dispersible microcapsules. A mixture of hexadecane and polyisobutylene was used as the inner solvent phase. Importantly, this eliminated the need for the deoxygenation step that is essential for preserving the triplets involved in the sTTA-UC process from the quenching by molecular oxygen, enabling a stable UC signal to be detected after a month of exposure to the ambient environment.[69] From this proof-of-concept work, the "encapsulated" sTTA-UC system has been developed significantly, resulting in the fabrication of complex and robust silica-coated capsules. The silica shell not only protects the included liquid upconverter from oxygen but also provides sites for further surface modification, which allows, when combined with its nanoscale dimension and structural rigidity, this sTTA-UC system to acquire various useful functionalities (Fig. 10). By decorating the upconverters silica shell with cadmium sulphide nanocrystals, as photocatalyst, and graphene oxide nanodisks, as a cocatalyst, Kim et al. demonstrated the photoassisted production of $\cdot$ OH and H_2O_2 using subbandgap photons. Considering that solar-powered H_2O_2 is not only a useful solar fuel but also a green oxidant and disinfectant for water purification, they suddenly spread the ensemble field of sTTA-UC applications, introducing new environment-related problems.[70,71]

In parallel, the development of UC-assisted PCWS devices did not stop. In particular, our group focused on the realization of multilayer devices with improved optical coupling between
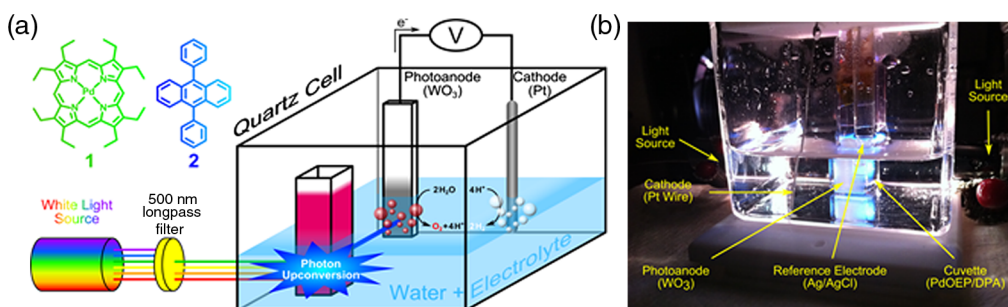

Fig. 9 (a) Chemical structures of the sensitizer PdOEP[1] and the emitter DPA[2] along with a schematic representation of a UC-powered photoelectrochemical cell relying on stochastic collection of photons. (b) Photograph of the UC-driven photoelectrochemical cell. Reproduced from Ref. 68 with permission from The Royal Society of Chemistry.
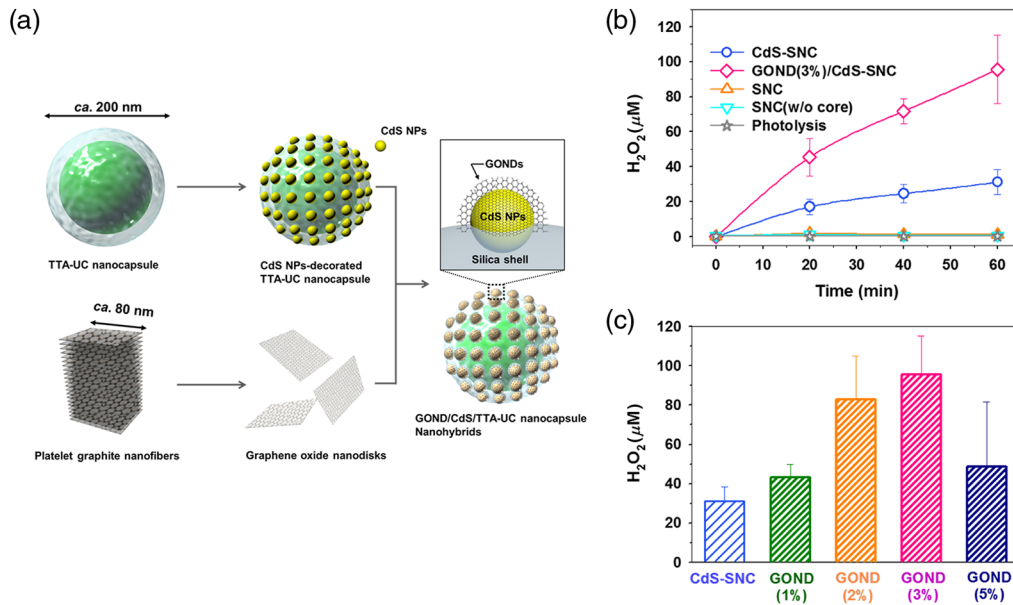
Fig. 10 (a) Schematic illustration of the sTTA-UC ternary nanohybrid preparation based on the selective graphene oxide nanodisk (GOND) wrapping of CdS nanoparticles attached on the surface of sTTA-UC nanocapsules. (b) Time-dependent profiles of H_2O_2 production on CdS–silica nanocapsules (CdS–SNC) and (GOND) (3 wt. %)/CdS–SNC. (c) H_2O_2 production as a function of the GOND content (wt. % versus CdS in CdS–SNC) in GOND/CdS–SNC hybrids (after 1-h reaction). All SNC, CdS–SNC, and GOND/CdS–SNC in (b) and (c) contain the chromophore pair of palladium(II) tetraphenyltetrabenzo-porphyrin (sensitizer) and 9,10-bis(phenylethynyl)anthracene (emitter) in their oleic acid core. Reproduced from Ref. 70 with permission from The Royal Society of Chemistry.

the PCWS cell and the UC system, to maximize the enhancement in the photocurrent and hydrogen production upon absorption of Vis photons. To realize a solid upconverter that can be easily implemented in the PCWS cell architecture, we propose the use of single-phase elastomers with low glass transitions temperature (<0°C) doped with proper dye pairs (Fig. 11).[21]

Due to the residual molecular diffusion provided by the soft host and to the reduced quenching of the involved metastable electronic excited states in a solid environment compared with a liquid one, we obtained efficient sTTA-UC at the solid state. Notably, due to the adhesive properties of the material, we were able to position the upconverter on the photoanode backside, where the subbandgap photons can be recovered properly and the upconverted photons
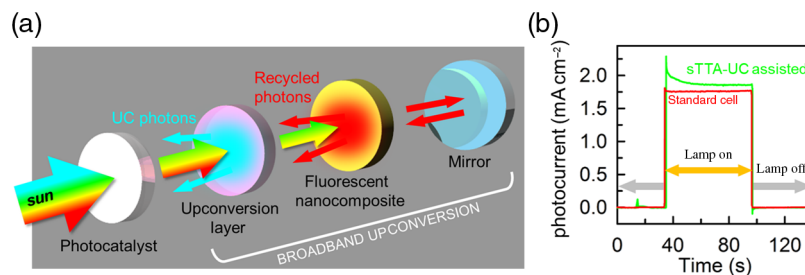

Fig. 11 (a) Architecture and optical properties of the UC-assisted water-splitting (UCA-WS) device, which exploits a metal oxide layer as the photocatalyst. The light passing through the photocatalyst is partially upconverted by the sTTA-UC layer to blue photons. The light transmitted through both the photocatalyst and the upconverter (yellow/green beam) is absorbed by the boosting layer (fluorescent nanocomposite) and recycled back to the sensitizer. An additional back-mirror completes the device to avoid optical losses. (b) Measurement of the photocurrent generated in the PCWS cell (red line) and in the UCS-WS device (green line) under 10 suns of excitation.
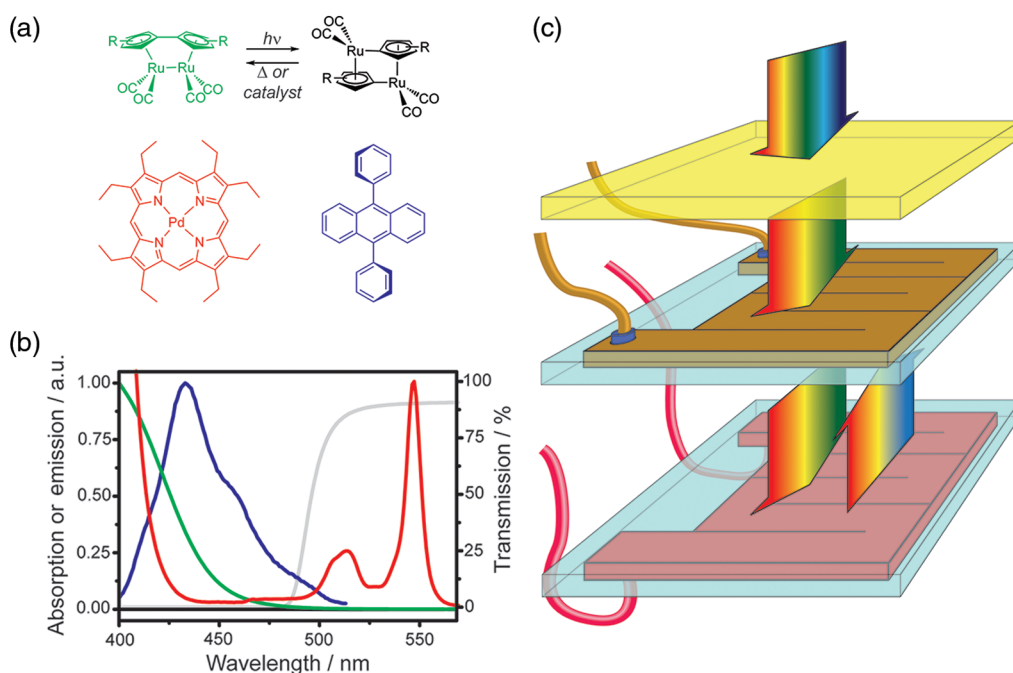
Fig. 12 (a) The FvRu$_2$ (green/black; $R =$ 1,1-dimethyltridecyl) used as a recyclable solar fuel and the sTTA-UC system based on the sensitizer PdOEP (red) and emitter DPA (blue). (b) Normalized absorption spectra of FvRu$_2$ (green/black) and PdOEP (red), fluorescence spectrum of DPA in the presence of PdOEP (blue), and transmission spectrum of the glass filter (gray, cut-on wavelength 495 nm). (c) A schematic picture of the microfluidic flow reactor. The white light traverses a glass filter to reach the microfluidic glass chips. The first chip contains the solar fuel and in the second one resides the sTTA-UC fluid. Reproduced from Ref. 73 with permission from The Royal Society of Chemistry.

harvested. By further developing this approach, we recently obtained the record enhancement of photocurrent generated in a standard PCWS cell under solar irradiance exploiting a sTTA-UC polymer boosted with highly fluorescent semiconductor nanocrystals, thus showing how the sTTA-UC materials can be successfully implemented in technologically relevant devices while matching the strict requirements of clean-energy production.[72]

Börjesson et al.[73] reported another example of a photochemical reaction enhanced by sTTA-UC, where the photoisomerization of a fulvalene diruthenium derivative (FvRu$_2$) was driven by blue photons upconverted from truncated white light. In the study, they set up a microfluidic system (Fig. 12) to enable the flowing of both the FvRu$_2$ containing liquid and the sTTA-UC fluid, consisting of DPA and PdOEP in toluene. They achieved a 130% increase in conversion of the photoisomer when coupled to the upconverter.

4 Conclusions

The aim of this review is to point out how the sTTA-UC began to be implemented in technologically appealing material and devices after its demonstration under solar light about a decade ago. Several strategies have been proposed to exploit the upconverted radiation. Therefore, several device architectures have been designed to implement the sTTA-UC mechanism in photovoltaic, photocatalytic, and photochemical systems, resulting in the realization of prototype devices that demonstrate the applicability of sTTA-UC. The results obtained indicate that the application of this UC mechanism to real-world devices demands the realization of more stable materials that are easy to integrate, for example, by embedding the upconverters in transparent matrices. It is important to point out that, considering the photophysics of the biexcitonic processes involved, the sTTA-UC should profit from the realization of structured and preorganized systems to enhance excitonic diffusivity and, therefore, promote TTA efficiency at ultralow

Table 1 Summary table of some state-of-the-art sTTA-UC pairs and working ranges.

Spectral range	Sensitizer	Emitter	$\lambda_{exc} - \lambda_{em}$ (nm)	References
Vis-to-UV	Biacetyl	PPO	442–360	74
	Ir(ppy)$_3$	pyrene	450–390	75
	4CzIPN	TP	450–343	76
Vis-to-Vis	PdOEP	DPA	544–435	35
	PtOEP	DPA	532–435	7
	ZnTPP	perylene	532–441	77
	PdDBA	perylene	532–470	53
	CdSe[a]	DPA	532–435	78
	PdTPBP	BPEA	633–515	35
	PdPh$_4$TBP	BPEA	635–515	35
	PdPh$_4$TBP	rubrene	635–560	79
NIR-to-Vis	PdPh$_4$OMe$_8$TNP	BPEN	695–560	35
	PdPc(OBu)8	rubrene	735–560	80
	PdTAP	rubrene	780–560	81
	OsPZn$_2$Os	rubrene	776–590	82
	PbSe[a]	rubrene	980–568	78
	PbS[a]	DBP	1010–612	23

[a]The systems where semiconductor nanocrystals are employed as sensitizers.

powers. This will enable reaching threshold intensities well below the solar irradiance, making sTTA-UC particularly suitable for application in real-life technologies.

However, an extra effort is still required to design and synthesize sTTA-UC materials. Table 1 summarizes some of the dye pairs currently known that are suitable for sTTA-UC and their spectral working range. It is easy to see that, while there is plenty of alternative pairs for Vis-to-Vis photon UC, the family of available materials for Vis-to-UV and NIR-to-Vis working ranges is significantly limited. Despite enormous progresses having been made on the design and architecture of sTTA-UC devices, this fundamental lack of materials is particularly detrimental for the evaluation of a reliable road-map evaluation for their commercial production. The use of semiconductor nanocrystals as sensitizers in substitution for the commonly employed metallated porphyrins was recently proposed,[23,78] opening the possibility of shifting the sTTA-UC working range toward the IR. However, the application of nanocrystals to sTTA-UC for solar technologies still has to be evaluated. Since nanocrystals lack transparency windows in the UC-emission spectral range, their reabsorption limits in principle their applicability to solar devices, where high optical densities are required. While the use of semiconductor nanocrystals may open the possibility to upconvert IR light, a striking strategy to produce UV upconverted photons still has to be found. The realization of efficient Vis-to-UV or, ideally, NIR-to-UV upconverters will indeed have a huge potential for photocatalytic and photochemical applications, but it would also greatly benefit other fields, such as photolithography and water sterilization.[83,84]

Disclosures

The authors declare no competing financial interests.

Acknowledgments

References

1. W. Shockley and H. J. Queisser, "Detailed balance limit of efficiency of p-n junction solar cells," *J. Appl. Phys.* **32**, 510–519 (1961).
2. T. F. Schulze and T. W. Schmidt, "Photochemical upconversion: present status and prospects for its application to solar energy conversion," *Energy Environ. Sci.* **8**, 103–125 (2015).
3. A. C. Atre and J. A. Dionne, "Realistic upconverter-enhanced solar cells with non-ideal absorption and recombination efficiencies," *J. Appl. Phys.* **110**, 034505 (2011).
4. T. Trupke, M. A. Green, and P. Würfel, "Improving solar cell efficiencies by up-conversion of sub-band-gap light," *J. Appl. Phys.* **92**, 4117–4122 (2002).
5. J. C. Goldschmidt and S. Fischer, "Upconversion for photovoltaics—a review of materials, devices and concepts for performance enhancement," *Adv. Opt. Mater.* **3**, 510–535 (2015).
6. R. R. Islangulov, D. V. Kozlov, and F. N. Castellano, "Low power upconversion using MLCT sensitizers," *Chem. Commun.* **2005**, 3776–3778 (2005).
7. S. Baluschev et al., "Up-conversion fluorescence: noncoherent excitation by sunlight," *Phys. Rev. Lett.* **97**, 143903 (2006).
8. V. Gray et al., "Triplet–triplet annihilation photon-upconversion: towards solar energy applications," *Phys. Chem. Chem. Phys.* **16**, 10345–10352 (2014).
9. W. Zou et al., "Broadband dye-sensitized upconversion of near-infrared light," *Nat. Photonics* **6**, 560–564 (2012).
10. T. W. Schmidt and F. N. Castellano, "Photochemical upconversion: the primacy of kinetics," *J. Phys. Chem. Lett.* **5**, 4062–4072 (2014).
11. Y. Y. Cheng et al., "Kinetic analysis of photochemical upconversion by triplet–triplet annihilation: beyond any spin statistical limit," *J. Phys. Chem. Lett.* **1**, 1795–1799 (2010).
12. N. Yanai and N. Kimizuka, "Recent emergence of photon upconversion based on triplet energy migration in molecular assemblies," *Chem. Commun.* **52**, 5354–5370 (2016).
13. S. Hoseinkhani et al., "Achieving the photon up-conversion thermodynamic yield upper limit by sensitized triplet–triplet annihilation," *Phys. Chem. Chem. Phys.* **17**, 4020–4024 (2015).
14. S. Baluschev et al., "Blue-green up-conversion: noncoherent excitation by NIR light," *Angew. Chem. Int. Ed.* **46**, 7693–7696 (2007).
15. T. N. Singh-Rachford, R. R. Islangulov, and F. N. Castellano, "Photochemical upconversion approach to broad-band visible light generation," *J. Phys. Chem. A* **112**, 3906–3910 (2008).
16. Y. Y. Cheng et al., "On the efficiency limit of triplet–triplet annihilation for photochemical upconversion," *Phys. Chem. Chem. Phys.* **12**, 66–71 (2010).
17. J. Sun et al., "Visible-light harvesting with cyclometalated iridium(III) complexes having long-lived ^{3}IL excited states and their application in triplet–triplet-annihilation based upconversion," *Eur. J. Inorg. Chem.* **2011**, 3165–3173 (2011).
18. A. Monguzzi et al., "Low power, non-coherent sensitized photon up-conversion: modelling and perspectives," *Phys. Chem. Chem. Phys.* **14**, 4322–4332 (2012).
19. T. Ogawa et al., "Highly efficient photon upconversion in self-assembled light-harvesting molecular systems," *Sci. Rep.* **5**, 10882 (2015).
20. A. Monguzzi et al., "Solid-state sensitized upconversion in polyacrylate elastomers," *J. Phys. Chem. C* **120**, 2609–2614 (2016).
21. A. Monguzzi et al., "High efficiency up-converting single phase elastomers for photon managing applications," *Adv. Energy Mater.* **3**, 680–686 (2013).
22. P. B. Merkel and J. P. Dinnocenzo, "Low-power green-to-blue and blue-to-UV upconversion in rigid polymer films," *J. Lumin.* **129**, 303–306 (2009).
23. M. Wu et al., "Solid-state infrared-to-visible upconversion sensitized by colloidal nano-crystals," *Nat. Photonics* **10**, 31–34 (2016).

24. A. Monguzzi, R. Tubino, and F. Meinardi, "Multicomponent polymeric film for red to green low power sensitized up-conversion," *J. Phys. Chem. A* **113**, 1171–1174 (2009).

25. A. Monguzzi et al., "Low-power-photon up-conversion in dual-dye-loaded polymer nano-particles," *Adv. Funct. Mater.* **22**, 139–143 (2012).

26. J.-H. Kim et al., "High efficiency low-power upconverting soft materials," *Chem. Mater.* **24**, 2250–2252 (2012).

27. J.-H. Kim and J.-H. Kim, "Encapsulated triplet–triplet annihilation-based upconversion in the aqueous phase for sub-band-gap semiconductor photocatalysis," *J. Am. Chem. Soc.* **134**, 17478–17481 (2012).

28. P. Duan, N. Yanai, and N. Kimizuka, "Photon upconverting liquids: matrix-free molecular upconversion systems functioning in air," *J. Am. Chem. Soc.* **135**, 19056–19059 (2013).

29. Z. Huang et al., "Nanocrystal size and quantum yield in the upconversion of green to violet light with CdSe and anthracene derivatives," *Chem. Mater.* **27**, 7503–7507 (2015).

30. S. Hisamitsu, N. Yanai, and N. Kimizuka, "Photon-upconverting ionic liquids: effective triplet energy migration in contiguous ionic chromophore arrays," *Angew. Chem. Int. Ed.* **54**, 11550–11554 (2015).

31. R. Vadrucci, C. Weder, and Y. C. Simon, "Organogels for low-power light upconversion," *Mater. Horiz.* **2**, 120–124 (2015).

32. F. Deng, W. Sun, and F. N. Castellano, "Texaphyrin sensitized near-IR-to-visible photon upconversion," *Photochem. Photobiol. Sci.* **13**, 813–819 (2014).

33. Y. V. Aulin et al., "Photochemical upconversion in metal-based octaethyl porphyrin-diphenylanthracene systems," *RSC Adv.* **5**, 107896–107903 (2015).

34. A. Monguzzi, R. Tubino, and F. Meinardi, "Upconversion-induced delayed fluorescence in multicomponent organic systems: role of Dexter energy transfer," *Phys. Rev. B* **77**, 155122 (2008).

35. R. R. Islangulov et al., "Noncoherent low-power upconversion in solid polymer films," *J. Am. Chem. Soc.* **129**, 12652–12653 (2007).

36. F. N. Castellano and T. N. Singh-Rachford, "Supra-nanosecond dynamics of a red-to-blue photon upconversion system," *Inorg. Chem.* **48**, 2541–2548 (2009).

37. A. Turshatov et al., "Room-temperature high-efficiency solid-state triplet–triplet annihilation up-conversion in amorphous poly(olefin sulfone)s," *ACS Appl. Mater. Interfaces* **9**, 8280–8286 (2017).

38. A. L. Hagstrom, F. Deng, and J.-H. Kim, "Enhanced triplet–triplet annihilation upconversion in dual-sensitizer systems: translating broadband light absorption to practical solid-state materials," *ACS Photonics* **4**, 127–137 (2017).

39. K. Sripathy et al., "Highly efficient photochemical upconversion in a quasi-solid organogel," *J. Mater. Chem. C* **3**, 616–622 (2015).

40. Y. Murakami et al., "Transparent and nonflammable ionogel photon upconverters and their solute transport properties," *J. Phys. Chem. B* **120**, 748–755 (2016).

41. P. Duan et al., "Photon upconversion in supramolecular gel matrixes: spontaneous accumulation of light-harvesting donor–acceptor arrays in nanofibers and acquired air stability," *J. Am. Chem. Soc.* **137**, 1887–1894 (2015).

42. R. Vadrucci, C. Weder, and Y. C. Simon, "Low-power photon upconversion in organic glasses," *J. Mater. Chem. C* **2**, 2837–2841 (2014).

43. S. H. Lee et al., "Light upconversion by triplet–triplet annihilation in diphenylanthracene-based copolymers," *Polym. Chem.* **5**, 6898–6904 (2014).

44. C. A. Parker and C. G. Hatchard, "Sensitized anti-stokes delayed fluorescence," *Proc. Chem. Soc.* 386–387 (1962).

45. M. J. Y. Tayebjee, D. R. McCamey, and T. W. Schmidt, "Beyond Shockley–Queisser: molecular approaches to high-efficiency photovoltaics," *J. Phys. Chem. Lett.* **6**, 2367–2378 (2015).

46. L. Frazer, J. K. Gallaher, and T. W. Schmidt, "Optimizing the efficiency of solar photon upconversion," *ACS Energy Lett.* **2**, 1346–1354 (2017).

47. Y. Y. Cheng et al., "Improving the light-harvesting of amorphous silicon solar cells with photochemical upconversion," *Energy Environ. Sci.* **5**, 6953–6959 (2012).

48. T. F. Schulze et al., "Efficiency enhancement of organic and thin-film silicon solar cells with photochemical upconversion," *J. Phys. Chem. C* **116**, 22794–22801 (2012).

49. T. F. Schulze et al., "Photochemical upconversion enhanced solar cells: effect of a back reflector," *Aust. J. Chem.* **65**, 480–485 (2012).

50. B. O'Regan and M. Gratzel, "A low-cost, high-efficiency solar cell based on dye-sensitized colloidal TiO_2 films," *Nature* **353**, 737–740 (1991).

51. B. E. Hardin, H. J. Snaith, and M. D. McGehee, "The renaissance of dye-sensitized solar cells," *Nat. Photonics* **6**, 162–169 (2012).

52. H. J. Snaith, "Estimating the maximum attainable efficiency in dye-sensitized solar cells," *Adv. Funct. Mater.* **20**, 13–19 (2010).

53. A. Monguzzi et al., "Efficient broadband triplet–triplet annihilation-assisted photon upconversion at subsolar irradiance in fully organic systems," *Adv. Funct. Mater.* **25**, 5617–5624 (2015).

54. A. Nattestad et al., "Dye-sensitized solar cell with integrated triplet–triplet annihilation upconversion system," *J. Phys. Chem. Lett.* **4**, 2073–2078 (2013).

55. J. O. Akindoyo et al., "Polyurethane types, synthesis and applications—a review," *RSC Adv.* **6**, 114453–114482 (2016).

56. C. Li et al., "Photocurrent enhancement from solid-state triplet–triplet annihilation upconversion of low-intensity, low-energy photons," *ACS Photonics* **3**, 784–790 (2016).

57. K. Terada et al., "Electric conduction properties of self-assembled monolayer films of Ru complexes with disulfide/phosphonate anchors in a Au–(molecular ensemble)–(Au nanoparticle) junction," *Chem. Lett.* **38**, 416–417 (2009).

58. S. P. Hill et al., "Photon upconversion and photocurrent generation via self-assembly at organic–inorganic interfaces," *J. Phys. Chem. Lett.* **6**, 4510–4517 (2015).

59. C. Simpson et al., "An intermediate band dye-sensitised solar cell using triplet–triplet annihilation," *Phys. Chem. Chem. Phys.* **17**, 24826–24830 (2015).

60. M. K. Nazeeruddin et al., "Conversion of light to electricity by cis-X2bis(2,2′-bipyridyl-4,4′-dicarboxylate)ruthenium(II) charge-transfer sensitizers (X = Cl-, Br-, I-, CN-, and SCN-) on nanocrystalline titanium dioxide electrodes," *J. Am. Chem. Soc.* **115**, 6382–6390 (1993).

61. S. P. Hill et al., "Integrated photon upconversion solar cell via molecular self-assembled bilayers," *ACS Energy Lett.* **1**, 3–8 (2016).

62. T. Dilbeck, S. P. Hill, and K. Hanson, "Harnessing molecular photon upconversion at sub-solar irradiance using dual sensitized self-assembled trilayers," *J. Mater. Chem. A* **5**, 11652–11660 (2017).

63. A. Luque and A. Martí, "Increasing the efficiency of ideal solar cells by photon induced transitions at intermediate levels," *Phys. Rev. Lett.* **78**, 5014–5017 (1997).

64. N. J. Ekins-Daukes and T. W. Schmidt, "A molecular approach to the intermediate band solar cell: the symmetric case," *Appl. Phys. Lett.* **93**, 063507 (2008).

65. Y. L. Lin et al., "Enhanced sub-bandgap efficiency of a solid-state organic intermediate band solar cell using triplet–triplet annihilation," *Energy Environ. Sci.* **10**, 1465–1475 (2017).

66. R. R. Islangulov and F. N. Castellano, "Photochemical upconversion: anthracene dimerization sensitized to visible light by a Ru[II] chromophore," *Angew. Chem. Int. Ed.* **45**, 5957–5959 (2006).

67. A. A. Ismail and D. W. Bahnemann, "Photochemical splitting of water for hydrogen production by photocatalysis: a review," *Sol. Energy Mater. Sol. Cells* **128**, 85–101 (2014).

68. R. S. Khnayzer et al., "Upconversion-powered photoelectrochemistry," *Chem. Commun.* **48**, 209–211 (2012).

69. A. Monguzzi et al., "Energy transfer enhancement by oxygen perturbation of spin-forbidden electronic transitions in aromatic systems," *Phys. Rev. B* **82**, 125113 (2010).

70. O. S. Kwon et al., "Triplet–triplet annihilation upconversion in CdS-decorated SiO_2 nanocapsules for sub-bandgap photocatalysis," *ACS Appl. Mater. Interfaces* **7**, 318–325 (2015).

71. H.-I. Kim et al., "Harnessing low energy photons (635 nm) for the production of H_2O_2 using upconversion nanohybrid photocatalysts," *Energy Environ. Sci.* **9**, 1063–1073 (2016).

72. A. Monguzzi et al., "Photocatalytic water splitting enhancement by sub-bandgap photon harvesting," *ACS Appl. Mater. Interfaces* (2017).

73. K. Börjesson et al., "Photon upconversion facilitated molecular solar energy storage," *J. Mater. Chem. A* **1**, 8521–8524 (2013).
74. T. N. Singh-Rachford and F. N. Castellano, "Low power visible-to-UV upconversion," *J. Phys. Chem. A* **113**, 5912–5917 (2009).
75. W. Zhao and F. N. Castellano, "Upconverted emission from pyrene and di-tert-butylpyrene using $Ir(ppy)_3$ as triplet sensitizer," *J. Phys. Chem. A* **110**, 11440–11445 (2006).
76. N. Yanai et al., "Increased vis-to-UV upconversion performance by energy level matching between a TADF donor and high triplet energy acceptors," *J. Mater. Chem. C* **4**, 6447–6451 (2016).
77. S. K. Sugunan et al., "Mechanisms of low-power noncoherent photon upconversion in metalloporphyrin-organic blue emitter systems in solution," *J. Phys. Chem. A* **113**, 8548–8556 (2009).
78. Z. Huang et al., "Hybrid molecule-nanocrystal photon upconversion across the visible and near-infrared," *Nano Lett.* **15**, 5552–5557 (2015).
79. S. Baluschev et al., "Upconversion with ultrabroad excitation band: simultaneous use of two sensitizers," *Appl. Phys. Lett.* **90**, 181103 (2007).
80. T. N. Singh-Rachford and F. N. Castellano, "Pd(II) phthalocyanine-sensitized triplet–triplet annihilation from rubrene," *J. Phys. Chem. A* **112**, 3550–3556 (2008).
81. V. Yakutkin et al., "Towards the IR limit of the triplet–triplet annihilation-supported upconversion: tetraanthraporphyrin," *Chemistry* **14**, 9846–9850 (2008).
82. J.-H. Olivier et al., "Near-infrared-to-visible photon upconversion enabled by conjugated porphyrinic sensitizers under low-power noncoherent illumination," *J. Phys. Chem. A* **119**, 5642–5649 (2015).
83. E. L. Cates, M. Cho, and J. H. Kim, "Converting visible light into UVC: microbial inactivation by Pr^{3+}-activated upconversion materials," *Environ. Sci. Technol.* **45**, 3680–3686 (2011).
84. F. Zhang, *Photon Upconversion Nanomaterials*, Springer-Verlag, Berlin (2016).

Jacopo Pedrini is a postdoctoral researcher at the University of Milano-Bicocca. He graduated in Materials Science in 2013. He was visiting PhD student at the Molecular Foundry at Berkeley Lab in Berkeley, California, USA and received his PhD in science and nanotechnology of materials from the University of Milano-Bicocca in 2017. His research focuses on molecular and inorganic nanomaterials for applications to renewable energies and photonics, including triplet-triplet annihilation based photon up-conversion for photovoltaics and bio-imaging.

Angelo Monguzzi is assistant professor at the University of Milano-Bicocca, where he received his PhD in materials science in 2008. His research concerns the photophysics of molecular semiconductors and nanomaterials, focusing on triplet–triplet annihilation-assisted upconversion for improving light-harvesting in solar devices. He authored more than 50 scientific papers. In 2014, he worked at the University of Kyushu, Japan, as JSPS fellow. From 2009 he was awarded several national and international prizes for young researchers.